European Review for Medical and Pharmacological Sciences 2019; 23: 2112-2124

Knockdown of MiR-140-5 promotes osteogenesis of adipose-derived mesenchymal stem cells by targeting TLR4 and BMP2 and promoting fracture healing in the atrophic nonunion rat model

P.-Y. GUO, L.-F. WU, Z.-Y. XIAO, T.-L. HUANG, X. LI

Orthopedics, First Affiliated Hospital of Kunming Medical University, Kunming, China

Abstract. – OBJECTIVE: This study aims to assess the effect and mechanism of genetically modified adipose-derived mesenchymal stem cells (ASCs) with recombinant lentiviruses mediated knockdown of miR-140-5p in ASCs' osteogenesis *in vitro* and atrophic nonunion rat model.

MATERIALS AND METHODS: This study included 36 male adult Sprague-Dawley (SD) rats weighing 400 g to 450 g from the experimental animal facility of our university. Approval was obtained from the University Animal Care Committee before the study. Rats' ASCs were prepared and genetically modified with lentivirus (Lv)-empty (NC) or Lv-miR-140-5p-TuD (inhibitors). After that, the expressions of RUNX2 and osteocalcin (OCN) were detected in the ASCs. To confirm the mechanisms of miR-140-5p in ASCs, we predicted the target genes by bioinformatics analysis and then the target genes were verified by luciferase reporting assay. The artificial atrophic nonunion was created in the rat's femoral bone. Animals were randomly divided into three groups according to the material implanted into bone defects space: AT scaffolds (AT group, n=12), AT scaffold with Lv-NC modified (AT+ASCs+Lv-NC group, n=12), AT scaffold with the Lv-miR-140-5p-TuD modified ASCs (AT+ASCs+Lv-miR-140-5p-TuD group, n=12). After four weeks, the rats were euthanized for the following radiographic examination, histologic study and biomechanical testing.

RESULTS: MiR-140-5p was down-regulated during osteogenic differentiation of ASCs, and inhibition of MiR-140-5p promoted osteogenesis of ASCs *in vitro*. Inhibition of MiR-140-5p promoted osteogenesis of ASCs and enhanced fracture in the atrophic nonunion rat model: AT+ASCs+Lv-NC group, AT+ASCs+Lv-miR-140-5p-TuD group resulted in a better bone formation and higher BMD and BMC than AT group, while excellent bone formation and the highest BMD and BMC were observed in AT+ASCs+Lv-miR-140-5p-TuD group. Both AT+ASCs+Lv-NC group and AT+ASCs+Lv-miR-140-5p-TuD group presented more mature characteristics in the micro-architecture than AT group, whereas AT+ASCs+Lv-miR-140-5p-TuD group presented the highest BV/TV, Tb.Th and Tb.N as well as the lowest Tb.Sp. The peak load of the operated femur increased by 94.43% AT+ASCs+Lv-miR-140-5p-TuD group, 50.68% in AT+ASCs+Lv-NC group compared to the control AT group, respectively. The result of luciferase reporting assay showed that miR-140-5p could directly target TLR4 and BMP2.

CONCLUSIONS: This study demonstrates that lentiviruses-mediated knockdown of miR-140-5p can significantly promote osteogenesis of ACSs by directly regulating its' target genes, TLR4 and BMP2, and that combined adipose scaffold with genetically modified ASCs can significantly enhance fracture-healing and bone formation in the atrophic nonunion rat model.

Key Words

Atrophic nonunion, Adipose scaffold, Adipose-derived stem cells, microRNA, Gene engineering, Bone regeneration.

Introduction

Although great advances in orthopedics have been achieved, there is a subset of fractures that continue to be deficient in bone regeneration and result in nonunion, which has become a great health issue[1,2]. In contrast to hypertrophic nonunion, the reasons for leading to atrophic nonunion have not been defined explicitly and the underlying mechanisms are still unknown. Bone regeneration is a complex and highly regulated process to restore the spatial arrangement of the skeletal system, and the failure of this process may lead to delayed healing or nonunion[3,4]. The repair of bone defects remains poor for the limited capacity of self-regeneration of bone[5]. The current "gold stan-

Corresponding Author: Xi Li, Ph.D; e-mail: 970244480@qq.com

dard" for surgical repair of bone defects involves the use of autologous bone, allograft bone, or artificial bone. However, these grafts present many limitations such as the immune rejection, morbidity at the donor sites, disease transmission, tissue matching, or difficult integration and survival of the transplanted tissue into the recipient materials[6-8]. Fortunately, with the development of bone tissue engineering techniques, there is an applicable alternative to achieve better effects[9]. Given that the process of bone regeneration in atrophic nonunion is complex, involving the bone-forming cells and environment, the combined application of scaffold, osteogenic growth factors, and the bone-forming cells or osteoblasts would act synergistically each other and would be a great advantage for bone regeneration therapies.

The bone-forming cells are the most important cells in the process of bone repair, and in these decades, adipose-derived mesenchymal stem cells (ASCs)-based cell therapy have attracted growing interest for their extensive capabilities of self-renewal and differentiation, and easy accessibility from adipose tissue by liposuction or resection[10,11]. Moreover, using ASCs as alternative to bone marrow-derived mesenchymal stem cells (BMSCs) would save patients from a very painful bone marrow aspiration, which can result in high donor site morbidity[12].

The bone-forming environment involves many factors. MicroRNAs (miRNAs) are approximately 22-nucleotide small non-coding RNAs, which can regulate the expression of multiple genes by specifically binding to the 3' non-coding region of their target mRNAs and thus participate in multiple biological processes[13]. In recent years, studies have demonstrated that various miRNAs exert an important regulatory effect on the osteogenesis and repairing bone defects[14,15]. Previous works found that MiR-140-5p, generated from the Mir140 gene, led to negatively osteogenic differentiation[16] and promotes adipocyte differentiation[17] of hMSCs. But there is little evidence about the role of miR-140-5p in ASCs' osteogenesis, and especially it's role in fracture-healing and bone formation of atrophic nonunion.

Moreover, scaffold is required in tissue engineering for bone regeneration and repair, to form a desired shape of the new bone, delivers the ASCs and other osteoinductive factors, in addition to providing temporary function and structure within bone defect[11]. Moreover, for fear of the potential of immunological rejection of foreign substances, the use of a self-tissue serving as the scaffold can be one of the choices[18,19].

Herein, we assessed the effect and mechanism of genetically modified ASCs with recombinant lentiviruses mediated knockdown of miR-140-5p in osteogenesis of ACSs, and further investigated whether seeded into adipose tissue (AT) scaffolds can enhance fracture-healing and bone formation in the atrophic nonunion rat model.

Materials and Methods

Preparation of ASCs

Human adipose-derived stem cells were purchased from the Scien-Cell Company (Carlsbad, CA, USA). The cells were cultured in growth medium consisting of Dulbecco's Modified Eagle's Medium (DMEM; Gibco, Rockville, MD, USA) supplemented with 10% fetal bovine serum (FBS; HyClone, GE Healthcare Life Science, South Logan, UT, USA) and 1% antibiotics (Gibco, Rockville, MD, USA) in an atmosphere of 5% CO_2 / 95% air at 37°C. Thereafter, the medium was changed every three days. All cell-based *in vitro* experiments were performed in triplicate.

Osteogenic Induction

To induce osteoblast differentiation, ASCs were plated in six-well plates (1×10^5 cells/well, 2 ml medium per well) and cultured normally. After five days cultivation (to 80-90% confluence), the media were replaced with the osteogenic medium (osteogenic medium kit was purchased from Millipore, Billerica, MA, USA) in an atmosphere of 5% CO_2/95% air at 37°C. Thereafter, the medium was changed every three days.

Recombinant Lentiviruses Construction, Amplification, and Transduction

Recombinant lentiviruses (Lv) were constructed using the Lv system (Invitrogen, Carlsbad, CA, USA). Production and purification of the recombinant Lv were performed as reported [18]. Briefly, we constructed the plasmid of anti-miR-140-5p by adopting RNA tough decoy (TuD) technique as previously described. EGFP, miR-140-5p inhibitor, and the corresponding negative control, were synthesized by Beijing Genomics Institute and subcloned into pET-32a (+) to yield Lv-NC, Lv-miR-140-5p. The resultant plasmid was transformed into *Escherichia coli* strain BL-21 based on the designed restriction enzyme sites. The recombinant Lv plasmid was selected on purimycin and confirmed by restriction endonuclease

digestion. The recombinant Lv plasmids were transduced into HEK293 cells where they were packaged into virus particles. Viral titers were estimated by optical density and standard plaque assay. Thus, 1×10^{10} particles/mL Lv were prepared. The transduction of ASCs with Lv was performed as reported[18]. ASCs were plated at a density of 10^6 cells/mL. Transductions of Lv at multiplicity of infection (MOI) of 25 were carried out. Polybrene was added to the culture at a concentration of 8 mg/mL. Twenty-four hours after the culture, the medium was replaced with fresh Dulbecco's Modified Eagle's Medium (DMEM) with 10% fetal bovine serum (FBS).

Western Blotting

Total protein was extracted from the ASCs, and the protein concentrations were measured using a bicinchoninic acid protein assay. A total of 80 mg denatured proteins were separated in 12.5% sodium dodecyl sulfate polyacrylamide gel electrophoresis (SDS-PAGE) and transferred onto nitrocellulose membrane. The membranes were then incubated with the antibodies (0.5-1 mg/mL) of anti-BMP2 (1:1000; Abcam, Invitrogen, Carlsbad, CA, USA), anti-TLR4 (1:500, Abcam, Invitrogen, Carlsbad, CA, USA), anti-RUNX2 (1:1000, Abcam, Invitrogen, Carlsbad, CA, USA), anti-OCN (1:500, Abcam, Invitrogen, Carlsbad, CA, USA), anti-GAPDH (1:1000; Abcam, Invitrogen, Carlsbad, CA, USA) and anti-β-actin (1:1000; Abcam, Invitrogen, Carlsbad, CA, USA) respectively, overnight at 4°C. The immunoreactive bands were visualized using enhanced chemiluminescence (Bio-Rad, Hercules, CA, USA) according to the manufacturer's instructions. The expression bands of target proteins were detected on a bioimaging system (VersaDoc MP 4000; Bio-Rad, Hercules, CA, USA), and the densitometric values were analyzed by ImageJ software. The housekeeping protein GAPDH or β-actin was used as an internal control.

Real-Time Quantitative Reverse Transcription Polymerase Chain Reaction (RT-PCR)

The total RNA was extracted from the ASCs using a RNeasy Mini kit. Total RNA was reverse transcribed using the SuperScript III kit (Invitrogen, Carlsbad, CA, USA), and quantitative reverse transcription polymerase chain reaction (RT-PCR) was performed using a polymerase chain reaction instrument (Opticon CFD-3200; MJ Research, Waltham, MA, USA). The primer sets included: BMP2: forward, TGAACACAGCTGGTCTCAGG; reverse, CTGGACTTAAGACGCTTCCG. TLR4: forward, CACCTAAGTGCGGAGAAA; reverse, GCAGTCACAGCGATACAAC. RUNX2: forward, TCTGGCCTTCCACTCTCAGT; reverse, GACTGGCGGGGTGTAAGTAA. Osteocalcin (OCN): forward, GCCGAGAAATGTTGGAGAAA; reverse, CTCCTTAATCTGGCCAACCA. β-actin: - forward, TCAGGTCATCACTATCGGCAAT; reverse, AAAGAAAGGGTGTAAAACCA. β-actin was used as the internal control, and the relative expression of amplified RNA samples was calculated using the $2^{-\Delta\Delta CT}$ method. All experiments were done in triplicate.

Femoral Atrophic Nonunion Model and Animal Experiment

Thirty-six male adult Sprague Dawley (SD) rats weighing 400 g to 450 g from the experimental animal facility of the authors' university were used in the study. Approval was obtained from the University Animal Care Committee before the study. All femoral atrophic nonunion model was performed according to a previously published protocol[20]. Animal experiments were as follows: briefly, rats were under general anesthesia with 3% sodium pentobarbital (1.5 mL/kg) and under sterile conditions. Then, a longitudinal lateral skin incision was made and the femur was exposed. The periosteum was destroyed by cauterization, and the muscles were carefully dissected from the bone 2 mm proximally and distally of the osteotomy. The external fixator[21] (Fa. M. Jagel, Bad Blankenburg, Germany) was attached to the femur using the fixator bar (29×5 mm) as a drill guide for the K-wires (d=1.25 mm). Approximately 2 mm segmental defect was made in the femoral bone with a 0.4 mm-thick diamond-cutting disk. The bone marrow was removed and a piece of abdominal wall adipose tissue was cut to fill up the bone defects. Next, animals were randomly divided into three groups: AT group, AT+ASCs+Lv-NC group, and AT+ASCs+Lv-miR-140-5p-TuD group. Transducing reagents were injected into four spots of the transplanted adipose tissue with 0.125 mL cells each spot. And the fixator bar was mounted at 10 mm to the mid-portion of the bone, and the wounds were closed. The animals were kept in separate cages with food and water under standard environmental condition with 12-h light/dark cycles and allowed to move freely throughout the experimental period. Inspection for clinical

signs of possible infection, evaluation for signs of discomfort, measurement of body weight and, if necessary, cleaning of the K-wire ducts with skin disinfectant, were performed once weekly. The rats were sacrificed 4 weeks after the surgery and subjected to the following assessments.

Biomechanical Testing

The samples for mechanical testing were stored at -20°C until the day of mechanical testing. The maximal anti-bending strength of the femoral bone was measured using an electronic universal material test machine (Zwick/RoellZ020, Kennesaw, GA, USA) with a 2 mm/min test motion speed. The load-displacement curve was recorded during the downward compression, and the ultimate load at failure (N; maximum force that the specimen sustained) calculated. The corresponding segments of non-operated contralateral femur were also measured as a normal control.

Radiographic Evaluation

The femur was harvested after sacrifice. Radiographs were taken, and then bone mineral density (BMD) and bone mineral content (BMC) of the region of interesting (ROI) were measured for each nonunion region using dual energy X-ray absorptiometry (DXA) analysis (Lunar iDXATM, GE Healthcare, Madison, WI, USA). The samples were scanned by a 2-mm thin-cut micro-CT scanner (μCT 40, Scanco Medical, Bassersdorf, Switzerland,) in an axial direction parallel to the long axis of the femur. The following micro-architecture parameters were assessed in VOI images: bone volume to total volume ratio (BV/TV), trabecular thickness (Tb.Th), trabecular separation (Tb.Sp), and trabecular number (Tb.N). BV/TV indicates the portion of mineralized tissue, and Tb.Th, Tb.Sp, and Tb.N provide detailed information on the thickness, organization and amount of trabeculae. All experimental data were sampled three times by an operator blinded to the experiment. After the above examinations, 6 samples were randomly selected from each group for histological examination. Other 6 samples were prepared for mechanical testing.

Histological Examination

6 samples were randomly selected from each group for histological examination and fixed in 4% paraformaldehyde solution for 24 h. After that, the samples were decalcified in 14.5% ethylenediaminetetraacetic acid buffer (pH = 7.2) for 6 weeks with solution change every 2 days; they were embedded in paraffin, sectioned into 5-mm sections with a microtome (Leica, Shanghai, China), and stained with for hematoxylin-eosin (H&E). Then, they were observed under a light microscope.

Statistical Analysis

Quantitative data with normal distribution is expressed as the mean ± standard deviation (SD) and compared using independent *t*-tests or 1-way or repeated-measures analysis of variance (ANOVA). All qualitative data are expressed as n (%) and compared using chi-square tests or Fisher's exact tests, which were used for correction if necessary. All *p*-values were 2-tailed and *p*-values less than 0.05 were considered statistically significant. For all statistical calculations, *p*-values were determined using SPSS (version 17.0 for Windows; SPSS Inc., Chicago, IL, USA). Tukey's post-hoc test was used to validate the analysis of variance (ANOVA) for comparing the data among groups.

Results

MiR-140-5p was Down-Regulated During Osteogenic Differentiation of ASCs

Under normal culture conditions on the fourth day, adipose-derived mesenchymal stem cells (ASCs) grew into spindle-shaped form, which morphology confirmed the ASCs phenotype (Figure 1A). Alkaline phosphatase (ALP) staining and Alizarin red staining (ARS) staining results showed that ASCs cultured in osteogenic induction medium for 14 days appeared obvious phenotype of osteoblast (Figure 1B). To explore the changes of miR-140-5p expression during ASCs differentiation into osteoblast or into adipocyte, qRT-PCR showed that the relative expression level of miR-140-5p was raised 7 days after adipogenic treatment of ASCs, while the level of miR-140-5p reduced 7 days after osteogenic treatment (compared with vehicle treatment group) (Figure 1C). And the relative expression level of miR-140-5p was significantly reduced at 7, and 14 days post-osteogenic-induction (compared with 0 day) (Figure 1D).

Inhibition of MiR-140-5p Promoted Osteogenesis of ASCs in Vitro

Knockdown of miR-140-5p in ASCs was achieved by infection with miR-140-5p-TuD (inhibitors) or empty (NC)-lentivirus expressing green fluorescent protein (GFP) (Figure 2A). Af-

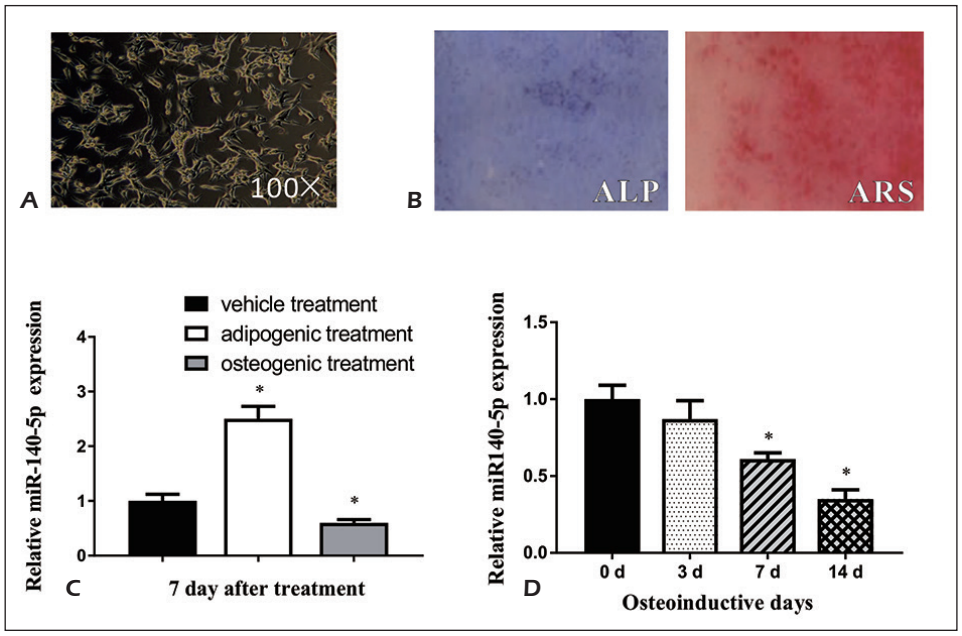

Figure 1. Expression of miR-140-5p in osteogenic differentiation. **A**, The Spindle shaped morphology of isolated from the abdominal subcutaneous fat *in vitro*. Microscopic multiple with 100×. **B**, 14 days after osteoinductive treatment, enhanced alkaline phosphatase (ALP) staining and Alizarin red staining (ARS) were observed, showing osteoblast differentiation of ASCs. **C**, qRT-PCR showed that the relative expression level of miR-140-5p was rised 7 days after adipogenic treatment of ASCs, while the level of miR-140-5p reduced 7 days after osteogenic treatment (compared with vehicle treatment group). **D**, The relative expression level of miR-140-5p was significantly reduced after osteogenic differentiation induction (compared with 0 day). *$p<0.05$.

ter gene transduction, we evaluated the expression of miR-140-5p in ASCs using qRT-PCR at 0, 3, 6, and 9 days, respectively. The expression of miR-140-5p in miR-140-5p-TuD-ASCs group was significantly lower than NC-ASCs (Figure 2B). After knockdown of miR-140-5p, the expression of osteogenesis-related genes, including Runx2 and OCN, was significantly enhanced at 3, 6, and 9 days compared with NC group (and 0 day), significantly upregulated, and gradually increased from day 3 to 9 (Figure 2C-E). Moreover, ALP and ARS staining at 14 days after transfection of lentivirus, showed significant increase of ALP and ARS activity in miR-140-5p-TuD group compared with these in NC group (Figure 2F). All the above results suggested that knockdown of miR-140-5p promotes osteogenesis of ASCs *in vitro*.

Inhibition of MiR-140-5p Promoted Osteogenesis of ASCs and Enhance Fracture in Atrophic Nonunion Rat Model

Femoral atrophic nonunion model was further used to verify the above results, and white arrow showed approximately 0.5 mm segmental defect was made in the femoral bone (Figure 3A). For biomechanical test, at 4 week, samples were prepared for mechanical testing, and the maximal anti-bending strength (Peak load) of the operated femoral bone was 73.23±4.55 N in AT group, 110.34±8.57 N in AT+ASCs+Lv-NC group, and 142.38±14.29 N in AT+ASCs+Lv-miR-140-5p-TuD group (Figure 2B). On the non-operated contralateral femur, there were no significant differences amongst the three groups in the mechanical property.

The femoral bone of the operated limbs was examined with X-ray, micro-CT, and histological examination, respectively (Figure 3C). All three groups showed a typical zone structure through the consolidation phase, and the newly trabeculae were formed in all three groups. There were two sclerotic zones proximally and distally adjacent to the central bone defects zone. Whereas AT+ASCs+Lv-miR-140-5p-TuD group showed complete bony union, and had the greatest radiographic density and the most mature regeneration bone in the bone defects zone. AT+ASCs+Lv-NC group showed partial emergence of both sclerotic zones with each other, but AT group showed no bony union in the bone defects.

For DXA examination, the BMD and BMC had significant differences between the AT group,

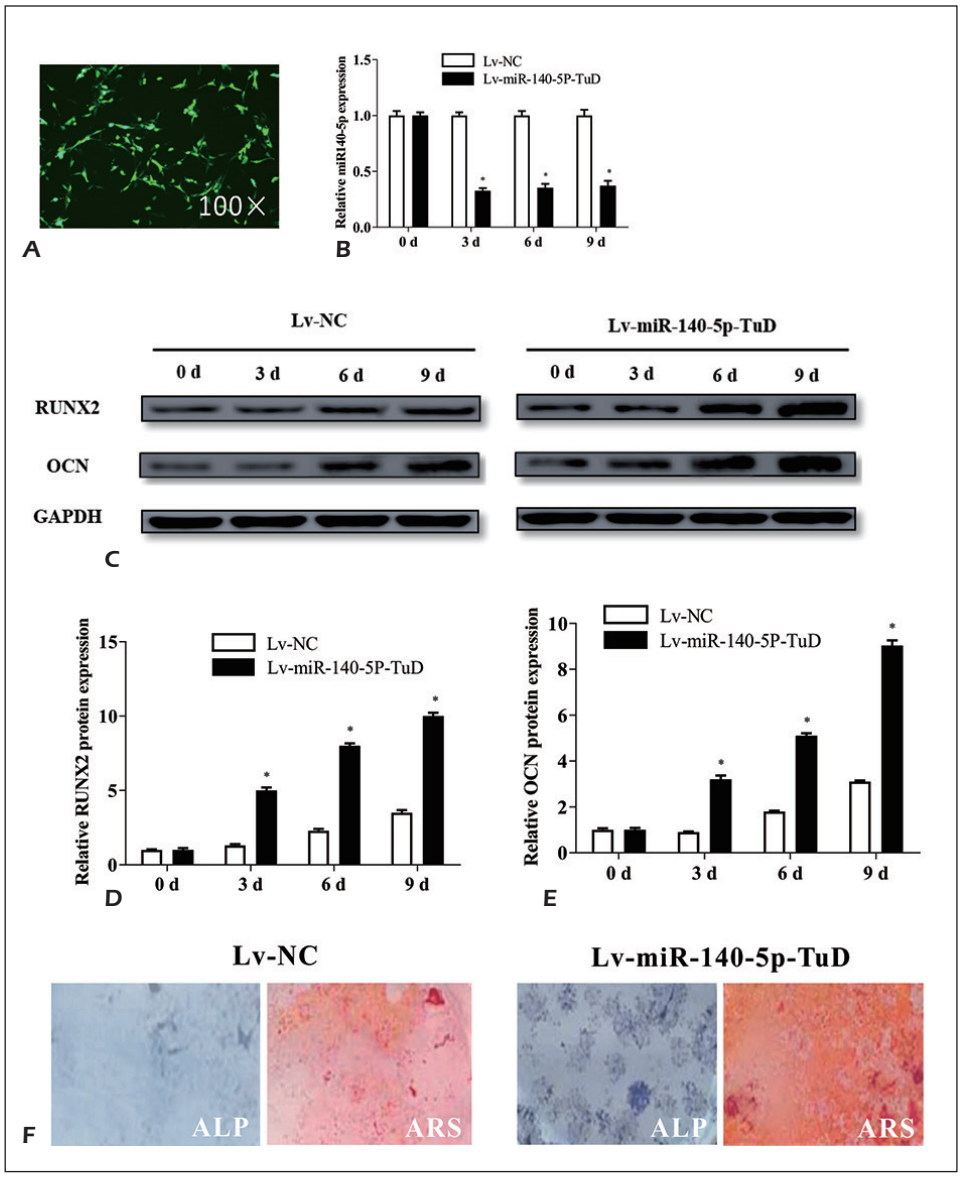

Figure 2. Inhibition of MiR-140-5p promoted osteogenesis of ASCs *in vitro*. **A**, The GFP positive ASCs after transfection. Microscopic multiple with 100×. **B**, qRT-PCR showed that the relative expression level of miR-140-5p was significant reduced in Lv-miR-140-5p-TuD group (compared with Lv-NC group). **C**, Osteobast-associated proteins, RUNX2 and OCN significantly increased after knockdown miR-140-5p (compared with Lv-NC group). Quantitative relative protein level of RUNX2 (**D**) and OCN (**E**). **F**, ALP and ARS staining assay results showed that knockdown of miR-140-5p significantly strengthen osteogenesis. *$p<0.05$.

AT+ASCs+Lv-NC group, and AT+ASCs+Lv-miR-140-5p-TuD group (for BMD, 402.64±22.64 g in AT group, 471.52±36.53 g in AT+ASCs+Lv-NC group, 598.64±46.38 g in AT+ASCs+Lv-miR-140-5p-TuD group; for BMC, 389.32±26.38 g in AT group, 466.67±34.21 g in AT+ASCs+Lv-NC group, 622.45±57.34 g in AT+ASCs+Lv-miR-140-5p-TuD group) (Figure 4A,B). On the non-operated contralateral femur, there were no significant differences among three groups in BMC and BMD.

Micro-CT examination illustrated the differences in microstructure in three groups. The AT group had significantly lower Tb.Th (0.07 mm ± 0.02 mm), BV/TV (7.62% ± 0.47%), and Tb.N (0.75 ± 0.14 mm^{-1}) as well as a significantly higher Tb.Sp (0.59 mm ± 0.12 mm) when compared to the other two groups. Moreover, AT+ASCs+Lv-miR-140-5p-TuD group exhibited the most mature characteristic in three groups, and with significantly higher BV/TV, Tb.Th and Tb.N compared

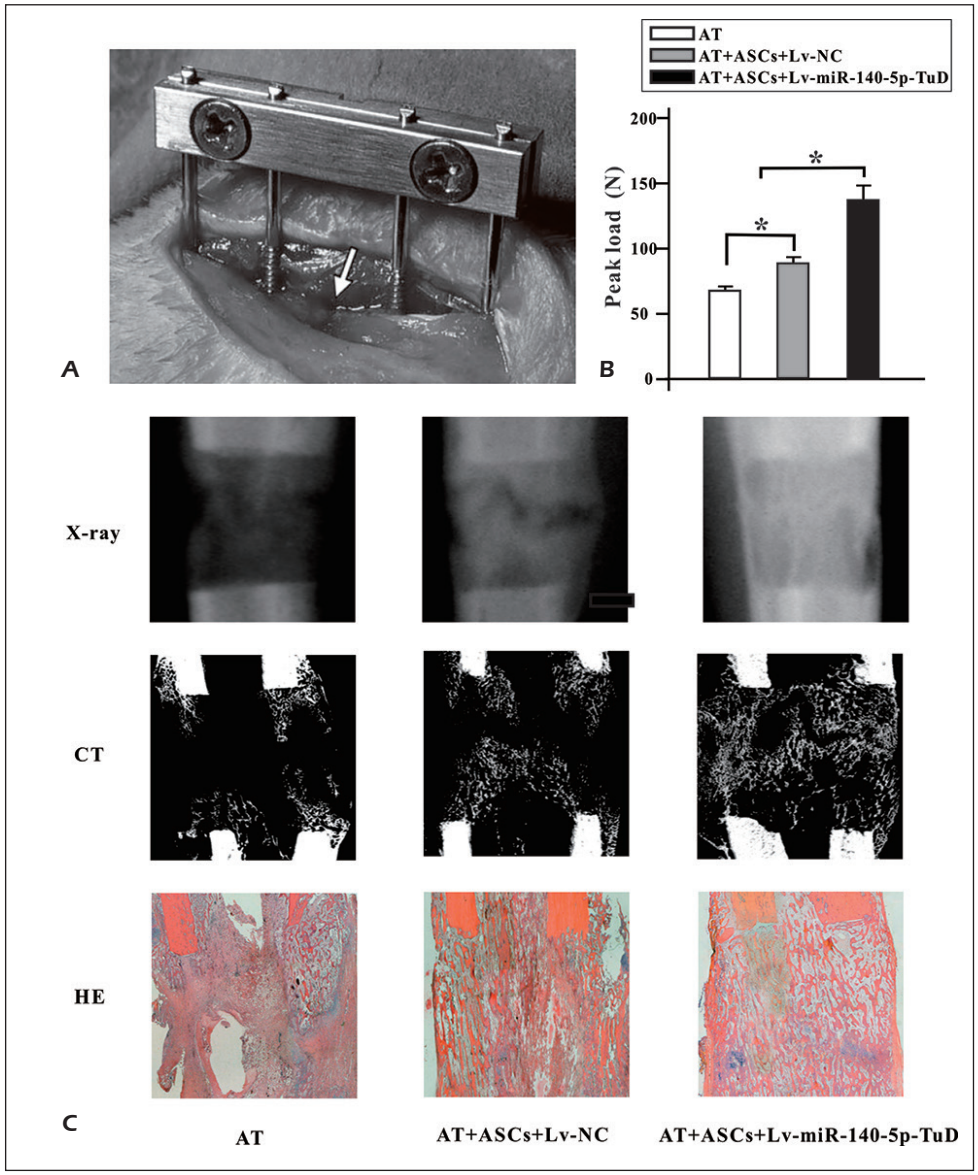

Figure 3. Femoral atrophic nonunion model and animal experiment. **A**, The external fixator in femoral atrophic nonunion model, and approximately 0.5 mm segmental defect was made in the femoral bone (*white arrow*). **B**, The peak load of the femoral bone was measured by three-point bending test. **C**, The X-ray, micro-CT, and histological appearances of the defects in femoral bone. *p<0.05.

with the AT+ASCs+Lv-NC group (for Tb.Th, 2.05-fold *vs.* 1.68-fold, p<0.05; for BV/TV, 4.41-fold *vs.* 1.81-fold, p<0.05; for Tb.N, 3.15-fold *vs.* 2.23-fold, p<0.05), whereas Tb.Sp was not significantly different between the two groups (for Tb.Sp, 0.46-fold *vs.* 0.53-fold) (Figure 4C-F).

TLR4 and BMP2 were the Directly Target Genes of MiR-140-5p

To found the mechanisms of inhibition of miR-140-5p promoted osteogenesis of ASCs, we performed bioinformatics analysis (microRNA.org). The relative expression level of TLR4 and BMP2 was significantly increased post-osteogenic-induction (p<0.05 compared with 0 day) (Figure 5A,B). Further, MiR-140-5p can bind to TLR4 and BMP2, and the binding site of miR-140-5p between TLR4 and BMP2 was predicted (Figure 5C-D) and confirmed by luciferase reporting assay. After 24 hours of transfection, we observed that the Luciferase activity was significantly lower in the group of overexpression miR-140-5p and wild-

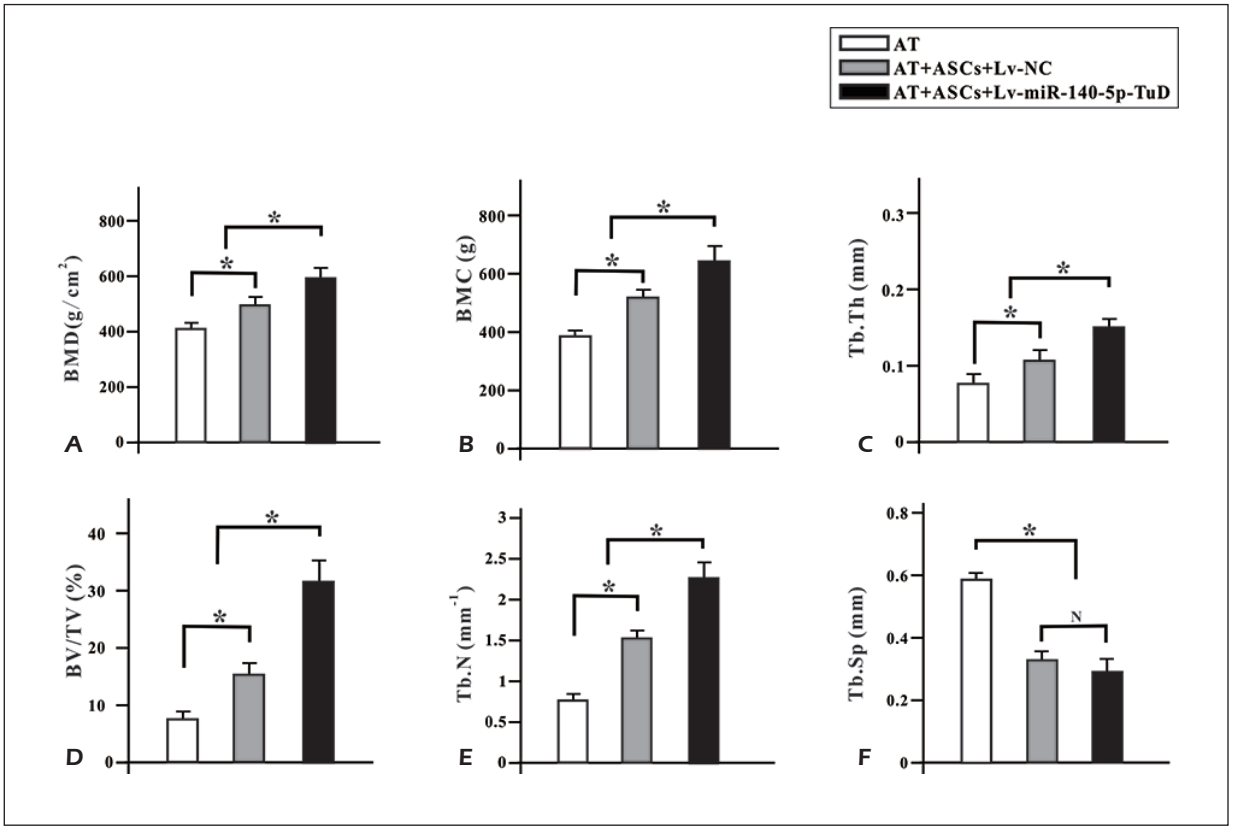

Figure 4. Parameters of radiographic evaluation in animal experiment. **A**, Bone mineral density (BMD) and (**B**) bone mineral content (BMC) of the nonunion region measured by Dual energy X-ray absorptiometry (DXA) analysis. (**C**) Bone volume to trabecular thickness (Tb.Th), (**D**) total volume ratio (BV/TV), (**E**) trabecular separation (Tb.Sp), and (**F**) trabecular number (Tb.N). *p<0.05.

type TLR4 and BMP2 than in the control group. However, after overexpression of miR-140-5p and mutant TLR4 and BMP2, no significant difference was found in the luciferase activity compared with the control group. This showed that the expression of Luciferase in gene was inhibited when miR-140-5p co-existed with the 3' UTR of both TLR4 and BMP2 (Figure 4E-F). The protein expression of TLR4 and BMP2 significantly declined, after overexpression of miR-140-5p (Figure 5G-H). Above results showed that TLR4 and BMP2 were the direct target genes of miR-140-5p.

Discussion

Although new technologies and advances in orthopedics surgery have been made, the atrophic nonunion of fractures, which may lead to morbidity and functional limitation for patients, is still a challenging and burning clinical problem [3]. The incidence of nonunion of fractures can be 5% to 20% and varies by fracture site[2,22,23]. The causes of nonunion are multifactorial and may be categorized by three key factors for bone regeneration: scaffold, osteogenic growth factors and the bone-forming cells or osteoblasts. And the therapeutic strategies aim is to correct these insufficient factors of osteogenesis[24]. Recently, researchers have been pointing to bone tissue engineering techniques with the combined application of all these factors of osteogenesis in the treatment of nonunions and in optimizing fracture-healing[2,3]. Our overall aim was to investigate the combined effects of adipose scaffold with gene engineering adult adipose-derived mesenchymal stem cells on fracture-healing and bone formation in atrophic nonunion.

Atrophic nonunion model in the rat femur proved to be useful for the study to evaluate new therapeutic strategies. By using an external fixation device, bone tissue engineering materials can be applied locally, and the process of healing can be

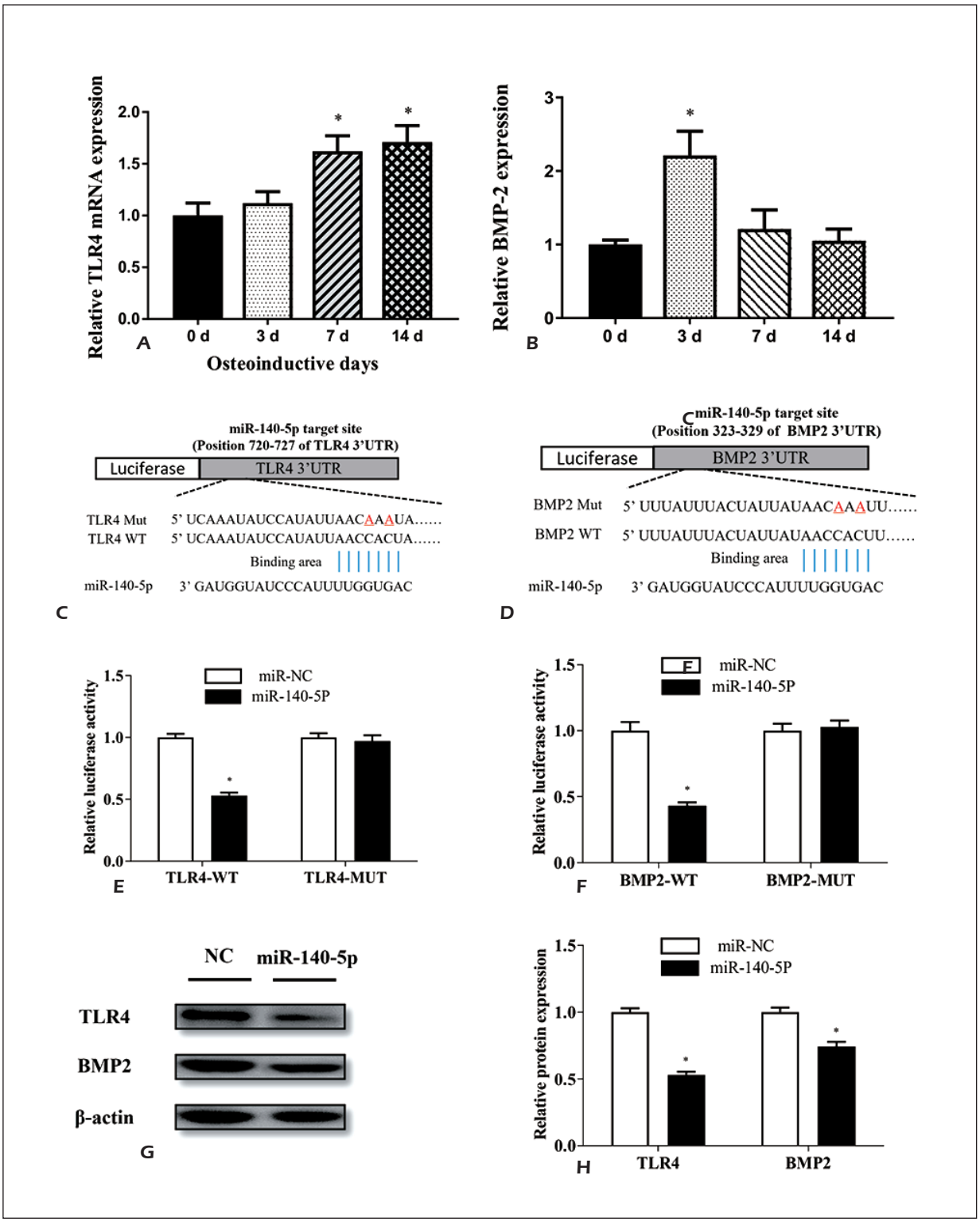

Figure 5. TLR4 and BMP2 were the directly target genes of MiR-140-5p. **A**, the relative expression level of TLR4 was significantly increased after osteogenesis (compared with 0 day). **B**, the relative expression level of BMP2 was significantly increased 3day after osteogenesis (compared with 0 day). **C**, The binding site of miR-140-5p to TLR4 is shown. **D**, The binding site of miR-140-5p to BMP2 is shown. **A**, Dual luciferase reporter gene assay of miR-140-5P and TLR4. **F**, Dual luciferase reporter gene assay of miR-140-5P and BMP2. Proteins levels of TLR4 (G) and BMP2 (H) significantly decreased after transfection with miR-140-5p. compared with Lv-NC group). *$p<0.05$.

investigated without suffering from interference of the implant[2,3]. In addition, choice of time points for investigating fracture-healing and bone formation was based on results of previous researches[18,25].

Many criteria have to be taken into consideration for choosing the source of bone-forming cells: the simplicity of harvest, morbidity at the donor site and the safety after implantation. The mesenchymal stem cells (MSCs) have gained worldwide attention for their success to be used in the field of orthopedics. The MSCs have several features for bone regeneration: the major natural healing cells involved during bone regeneration, their immune-privileged feature, and their ability to secrete immunomodulatory and other factors with therapeutic utility. Bone marrow-derived MSCs (BMSCs) have been the choice in stem cell therapy, thus far, for bone regeneration. However, it has been confirmed that adipose-derived stem cells (ASCs) have similar morphology, immunophenotype, multilineage potential, and transcriptome compared to BMSCs. And ACSs are promising for their extensive capabilities of self-renewal and differentiation, lower donor morbidity and easy accessibility from adipose tissue by liposuction or resection[11,26]. Moreover, the BMSCs failed to repair mandible defects[27], but ASCs succeeded to improve maxilla[28] and calvarial[29] bone repair. Therefore, ASCs should be better alternatives to BMSCs as source of bone-forming cells in this study.

Many authors have found that miRNA can alter the osteogenic ability of various types of human cells by regulating the expression level of target genes[30,31]. For example, Su et al[32] showed that miR-26a targets GSK3-beta and SMAD1 genes to regulate Wnt/ BMP signal transduction pathways, which can significantly affect the osteogenic differentiation of MSCs and adipose stem cells (ADSCs). And miR-140-5p has been identified as an enriched miRNA undifferentiated hMSCs which negatively regulates the osteogenic lineage commitment and that the expression levels of miR-140-5p were dynamically regulated during osteogenic differentiation[16]. Moreover, miR-140-5p promotes adipocyte differentiation by targeting transforming growth factor-β signaling[17]. These previous studies in BMSCs are consistent with our findings in ASCs. We found that the expression of miR-140-5p was decreased during osteogenesis of ASCs, suggesting inhibition of miR-140-5p might promote the osteogenesis of ASCs. To confirm this hypothesis, in this study, ASCs were genetically modified with Lv-miR-140-5p-TuD to inhibit the expression of miR-140-5p *in vitro*. Our results revealed that genetic inhibition of miR-140-5p increased the expression of signature molecules of osteogenesis, RUNX2 and OCN[33-35]. Moreover, the ALP and ARS staining results also indicated that inhibition of miR-140-5p promoted osteogenesis of ASCs *in vitro*. More importantly, their role in fracture-healing and bone formation of atrophic nonunion had not been investigated in previous studies. Thus, we investigate the ASCs genetically modified with Lv-miR-140-5p-TuD, on fracture-healing and bone formation in atrophic nonunion (Figure 6). To use gene-engineering ASCs to repair bone defects, scaffolds are necessary. Using self-material in bone repair can avoid immune rejection and the present study used self-adipose pad in the bone defect repairing with an encouraging result[18]. Thus, genetically modified ASCs were seeded into adipose tissue (AT) scaffolds. At the 4th week, both radiographic and histological examinations showed that all three groups had the newly formed trabeculae and typical zone structure through the consolidation phase, but AT+ASCs+Lv-miR-140-5p-TuD group displayed complete bony union, the greatest radiographic density and the most mature regeneration bone in the bone defects zone. AT+ASCs+Lv-NC group manifested partial emergence of both sclerotic zones with each other, but AT group showed no bony union and focal defects in the bone defects. Meanwhile, significantly highest BMC, BMD, BV/TV, Tb.Th, Tb.N and Peak load had been shown in AT+ASCs+Lv-miR-140-5p-TuD group, compared to other two groups. Significantly higher BMC, BMD, BV/TV, Tb.Th, Tb.N and Peak load had been found in AT+ASCs+Lv-NC group compared to AT group. Moreover, significantly lower Tb.Sp was found in AT+ASCs+Lv-NC group and AT+ASCs+Lv-miR-140-5p-TuD group, compared to AT group. These findings implicate the feasibility and potential of using ACSs with genetically inhibition of miR-140-5p to induce bone formation and fracture-healing. Our results are consistent with previous gene-modified ASCs transplantation studies. Li et al[18] also confirmed that using adipose scaffold and gene-modified ASCs transplantation can promote bone formation and bone defects repair[18].

To establish the regulatory mechanisms that control osteogenesis of ACS by miR-140-5p, we performed bioinformatics analysis (microRNA.org, Targetscan, and miRDB). The binding site of miR-140-5p was predicted; miR-140-5p can bind to the site 720-727 of TLR4 3'TUR and 323-329

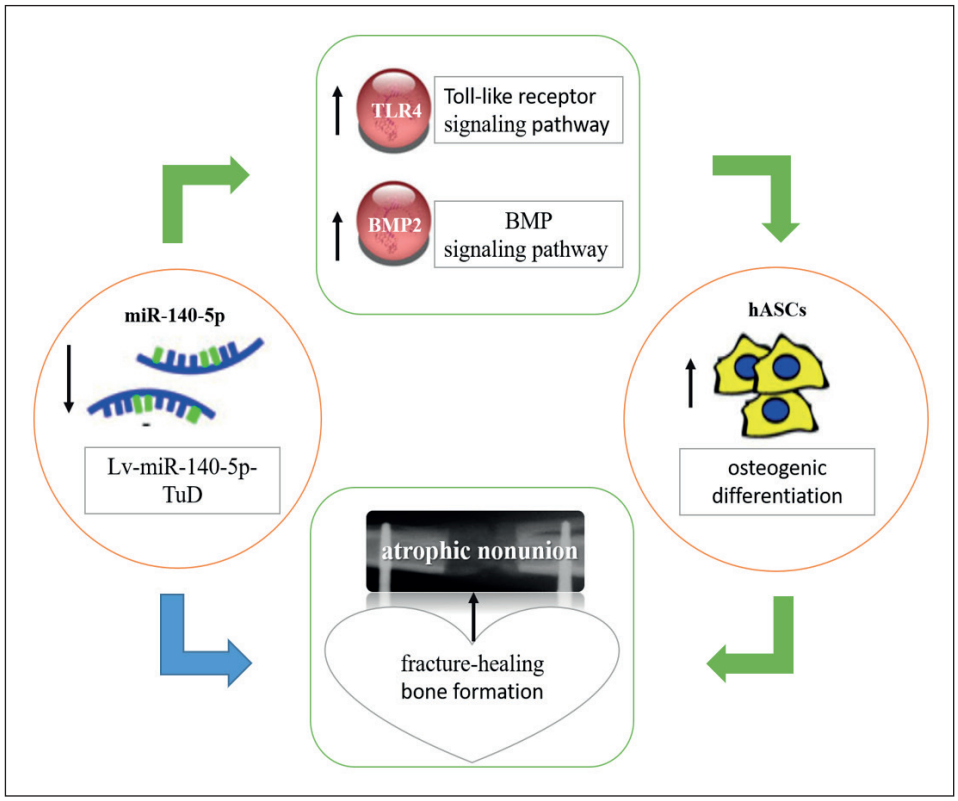

Figure 6. A proposed schematic diagram of miR-140-5p-TLR4/BMP2 axis in ASCs' osteogenesis *in vitro* and in atrophic nonunion rat model.

of BMP2 3'TUR. In addition, BMP-2, as osteogenic growth factor, was known to enhance the osteogenic potency of MSCs through BMP signal pathway [36-38]. Interestingly, TLR4 could promote osteogenic differentiation of ASCs via Toll-like receptor (TLR) signaling pathway[39]. The luciferase assay in our study also showed that miR-140-5p altered the luciferase activity of the 3' -UTR reporters of TLR4 and BMP2, suggesting they are the direct targets of miR-140-5p.

However, the direct evidence *in vivo* comparison between ASCs and BMSCs in bone regeneration is lacking[11]. And it is urgent for experiments to clarify which stem cells are prior or what specific condition should be used in order to improve the reliability and outcome of stem cells therapy in orthopedics.

Conclusions

We demonstrated that lentiviruses-mediated knockdown of miR-140-5p can significantly promote osteogenesis of ACSs, and combined adipose scaffold with genetically modified ASCs can significantly enhance fracture-healing and bone formation in atrophic nonunion rat model. Also, the mechanism of miR-140-5p in ACSs' osteogenesis was directly regulating its' target genes, TLR4 and BMP2. These findings implicate recombinant lentiviruses-mediated knockdown of miR-140-5p therapy can improve bone healing. The results also support the feasibility of using ACSs to induce bone formation and fracture-healing.

Conflict of Interests

The authors have no conflicts of interest or financial ties to disclose.

References

1) Tzioupis C, Giannoudis PV. Prevalence of long-bone non-unions. Injury 2007; 38 Suppl 2: S3-S9.
2) Bell A, Templeman D, Weinlein JC. Nonunion of the femur and tibia: an update. Orthop Clin North Am 2016; 47: 365-375.
3) Tseng SS, Lee MA, Reddi AH. Nonunions and the potential of stem cells in fracture-healing. J Bone Joint Surg Am 2008; 90 Suppl 1: 92-98.

4) Kokubu T, Hak D J, Hazelwood SJ, Reddi AH. Development of an atrophic nonunion model and comparison to a closed healing fracture in rat femur. J Orthop Res 2003; 21: 503-510.
5) Watanabe Y, Arai Y, Takenaka N, Kobayashi M, Matsushita T. Three key factors affecting treatment results of low-intensity pulsed ultrasound for delayed unions and nonunions: instability, gap size, and atrophic nonunion. J Orthop Sci 2013; 18: 803-810.
6) Conway JD. Autograft and nonunions: morbidity with intramedullary bone graft versus iliac crest bone graft. Orthop Clin North Am 2010; 41: 75-84.
7) Li L, Neligan PC. [Anterolateral thigh perforator free flaps for reconstruction of head and four limb soft tissue defects after tumor resection]. Zhongguo Xiu Fu Chong Jian Wai Ke Za Zhi 2007; 21: 340-342.
8) Khan SN, Cammisa FP Jr, Sandhu HS, Diwan AD, Girardi FP, Lane JM. The biology of bone grafting. J Am Acad Orthop Surg 2005; 13: 77-86.
9) Crane GM, Ishaug SL, Mikos AG. Bone tissue engineering. Nat Med 1995; 1: 1322-1324.
10) Gimble JM, Katz AJ, Bunnell BA. Adipose-derived stem cells for regenerative medicine. Circ Res 2007; 100: 1249-1260.
11) Monaco E, Bionaz M, Hollister SJ, Wheeler MB. Strategies for regeneration of the bone using porcine adult adipose-derived mesenchymal stem cells. Theriogenology 2011; 75: 1381-1399.
12) Bredeson C, Leger C, Couban S, Simpson D, Huebsch L, Walker I, Shore T, Howson-Jan K, Panzarella T, Messner H, Barnett M, Lipton J. An evaluation of the donor experience in the Canadian multicenter randomized trial of bone marrow versus peripheral blood allografting. Biol Blood Marrow Transplant 2004; 10: 405-414.
13) Ge DW, Wang WW, Chen HT, Yang L, Cao XJ. Functions of microRNAs in osteoporosis. Eur Rev Med Pharmacol Sci 2017; 21: 4784-4789.
14) Deng Y, Zhou H, Zou D, Xie Q, Bi X, Gu P, Fan X. The role of miR-31-modified adipose tissue-derived stem cells in repairing rat critical-sized calvarial defects. Biomaterials 2013; 34: 6717-6728.
15) Ge JB, Lin JT, Hong HY, Sun YJ, Li Y, Zhang CM. MiR-374b promotes osteogenic differentiation of MSCs by degrading PTEN and promoting fracture healing. Eur Rev Med Pharmacol Sci 2018; 22: 3303-3310.
16) Hwang S, Park S, Lee HY, Kim SW, Lee JS, Choi EK, You D, Kim CS, Suh N. miR-140-5p suppresses BMP2-mediated osteogenesis in undifferentiated human mesenchymal stem cells. FEBS Lett 2014; 588: 2957-2963.
17) Zhang X, Chang A, Li Y, Gao Y, Wang H, Ma Z, Li X, Wang B. miR-140-5p regulates adipocyte differentiation by targeting transforming growth factor-β signaling. Sci Rep 2015; 5: 18118.
18) Li W, Fan J, Chen F, Yang W, Su J, Bi Z. Construction of adipose scaffold for bone repair with gene engineering bone cells. Exp Biol Med (Maywood) 2013; 238: 1350-1354.
19) Toupadakis CA, Wong A, Genetos DC, Cheung WK, Borjesson DL, Ferraro GL, Galuppo LD, Leach JK, Owens SD, Yellowley CE. Comparison of the osteogenic potential of equine mesenchymal stem cells from bone marrow, adipose tissue, umbilical cord blood, and umbilical cord tissue. Am J Vet Res 2010; 71: 1237-1245.
20) Kaspar K, Matziolis G, Strube P, Sentürk U, Dormann S, Bail HJ, Duda GN. A new animal model for bone atrophic nonunion: fixation by external fixator. J Orthopaedic Res 2008; 26: 1649-1655.
21) Kaspar K, Schell H, Toben D, Matziolis G, Bail HJ. An easily reproducible and biomechanically standardized model to investigate bone healing in rats, using external fixation. Biomed Tech (Berl) 2007; 52: 383-390.
22) Einhorn TA. Enhancement of fracture-healing. J Bone Joint Surg Am 1995; 77: 940-956.
23) Marsh D. Concepts of fracture union, delayed union, and nonunion. Clin Orthop Relat Res 1998 (355 Suppl): S22-S30.
24) Gómez-Barrena E, Rosset P, Lozano D, Stanovici J, Ermthaller C, Gerbhard F. Bone fracture healing: cell therapy in delayed unions and nonunions. Bone 2015; 70: 93-101.
25) Li W, Zara JN, Siu RK, Lee M, Aghaloo T, Zhang X, Wu BM, Gertzman AA, Ting K, Soo C. Nell-1 enhances bone regeneration in a rat critical-sized femoral segmental defect model. Plast Reconstr Surg 2011; 127: 580-587.
26) Bahney CS, Miclau T. Therapeutic potential of stem cells in orthopedics. Indian J Orthop 2012; 46: 4-9.
27) Meijer GJ, de Bruijn JD, Koole R, van Blitterswijk CA. Cell based bone tissue engineering in jaw defects. Biomaterials 2008; 29: 3053-3061.
28) Kulakov AA, Goldshtein DV, Grigoryan AS, Rzhaninova AA, Alekseeva IS, Arutyunyan IV, Volkov AV. Clinical study of the efficiency of combined cell transplant on the basis of multipotent mesenchymal stromal adipose tissue cells in patients with pronounced deficit of the maxillary and mandibulary bone tissue. Bull Exp Biol Med 2008; 146: 522-525.
29) Levi B, James AW, Nelson ER, Vistnes D, Wu B, Lee M, Gupta A, Longaker MT. Human adipose derived stromal cells heal critical size mouse calvarial defects. PLoS One 2010; 5: e11177.
30) Taipaleenmaki H, Bjerre HL, Chen L, Kauppinen S, Kassem M. Mechanisms in endocrinology: micro-RNAs: targets for enhancing osteoblast differentiation and bone formation. Eur J Endocrinol 2012; 166: 359-371.
31) Hao W, Liu H, Zhou L, Sun Y, Su H, Ni J, He T, Shi P, Wang X. MiR-145 regulates osteogenic differentiation of human adipose-derived mesenchymal stem cells through targeting FoxO1. Exp Biol Med (Maywood) 2018; 243: 386-393.
32) Su X, Liao L, Shuai Y, Jing H, Liu S, Zhou H, Liu Y, Jin Y. MiR-26a functions oppositely in osteogenic differentiation of BMSCs and ADSCs depending on distinct activation and roles of Wnt and BMP signaling pathway. Cell Death Dis 2015, 6: e1851.
33) Li Y, Ge C, Long JP, Begun DL, Rodriguez JA, Goldstein SA, Franceschi RT. Biomechanical stimulation of osteoblast gene expression requires phosphorylation of the RUNX2 transcription factor. J Bone Miner Res 2012; 27: 1263-1274.
34) Moshaverinia A, Ansari S, Chen C, Xu X, Akiyama K, Snead ML, Zadeh HH, Shi S. Co-encapsulation of anti-BMP2 monoclonal antibody and mesenchymal stem cells in alginate microspheres for bone tissue engineering. Biomaterials 2013; 34: 6572-6579.

35) Wohl GR, Towler DA, Silva MJ. Stress fracture healing: fatigue loading of the rat ulna induces upregulation in expression of osteogenic and angiogenic genes that mimic the intramembranous portion of fracture repair. Bone 2009; 44: 320-330.
36) Sakou T. Bone morphogenetic proteins: from basic studies to clinical approaches. Bone 1998, 22: 591-603.
37) Li G, Bouxsein ML, Luppen C, Li XJ, Wood M, Seeherman HJ, Wozney JM, Simpson H. Bone consolidation is enhanced by rhBMP-2 in a rabbit model of distraction osteogenesis. J Orthop Res 2002; 20: 779-788.
38) Issa J P, Do NC, Lamano T, Iyomasa MM, Sebald W, de Albuquerque RF Jr. Effect of recombinant human bone morphogenetic protein-2 on bone formation in the acute distraction osteogenesis of rat mandibles. Clin Oral Implants Res 2009; 20: 1286-1292.
39) Yu L, Qu H, Yu Y, Li W, Zhao Y, Qiu G. LncRNA-PCAT1 targeting miR-145-5p promotes TLR4-associated osteogenic differentiation of adipose-derived stem cells. J Cell Mol Med 2018; 22: 6134-6147.